Supporting Information

Background-filtered telomerase activity assay with cyclic DNA cleavage amplification

Hyogu Han,[ab] Chihyun Park,[c] Chang Yeol Lee[d] and Jun Ki Ahn*[a]*

[a] Material & Component Convergence R&D Department, Korea Institute of Industrial Technology (KITECH), Ansan, 15588, Korea

[b] Department of Chemistry, Gangneung-Wonju National University, Gangneung, 25457, Korea

[c] Daejeon District Office, National Forensic Service, Daejeon, 34054, Korea

[d] Bionanotechnology Research Center, Korea Research Institute of Bioscience and Biotechnology (KRIBB), Daejeon, 34141, Korea

*Corresponding author.

Tel.: +82-42-860-4456; Fax: +82-42-861-1759

E-mail address: lcyeol8457a@kribb.re.kr (C.Y. Lee).

Tel.: +82-31-8040-6391; Fax: +82-31-8040-6220

E-mail address: jkahn@kitech.re.kr (J.K. Ahn).

Fig S1. QUEST reaction at 37 °C. FEN1 was active enough to result in high signal for the pre-concatenated TSP (100 nM) (Signal-to-noise ratio (SNR) = 32.4). Pre-concatenated TSP is TSP appended with telomeres ($(TTAGGG)_{12}$) (Table S2).

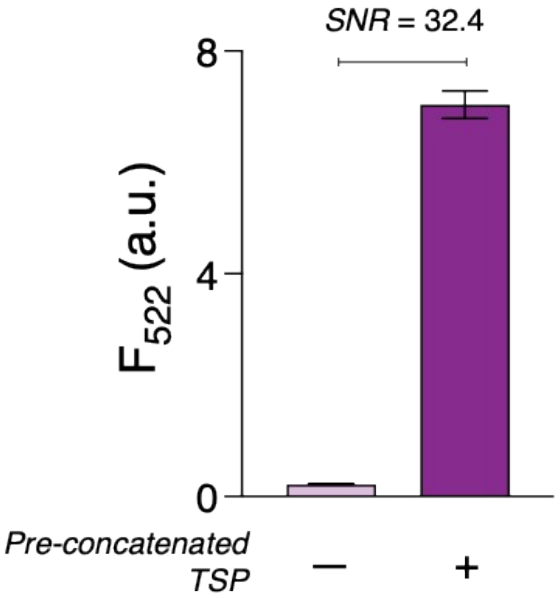

Though FEN1 is known to have the optimal activity at 65 °C, it retained significant activity even at 37 °C as evidenced by high SNR (32.4). This is consistent with the previous literatures.[1–4]

Fig. S2. Verification of FEN1-catalyzed cyclic cleavage reaction. (a) Compared to the one-to-one cleavage reaction, where a single cleavage event of RP-Q/F takes place for a single pre-concatenated TSP_{mini}, the FEN1-catalyzed cyclic cleavage reaction induces multiple cleavage reactions on RP-Q/F. Intact RP-Q/F displaces the cleaved RP-Q/F to initiate another round of cleavage reaction, thereby switching on a number of fluorophores. (b) Oligonucleotide sequences used in the experimental verification of FEN1-catalyzed cyclic cleavage reaction. (c) The result supported the cyclic cleavage reaction of FEN1. Signals (ΔF) of the FEN1-catalyzed reaction were significantly higher than those of controls in which concentration-matched RP_{cut}-F samples were included to assume the one-to-one cleavage reaction (*$p < 0.005$). RP_{cut}-F is the expected form of cleaved RP-Q/F. $\Delta F = F - F_0$, where F_0 is the fluorescence signal in the absence of pre-concatenated TSP_{mini} (in FEN1-catalyzed reaction) or RP_{cut}-F (in Control) at 522 nm.

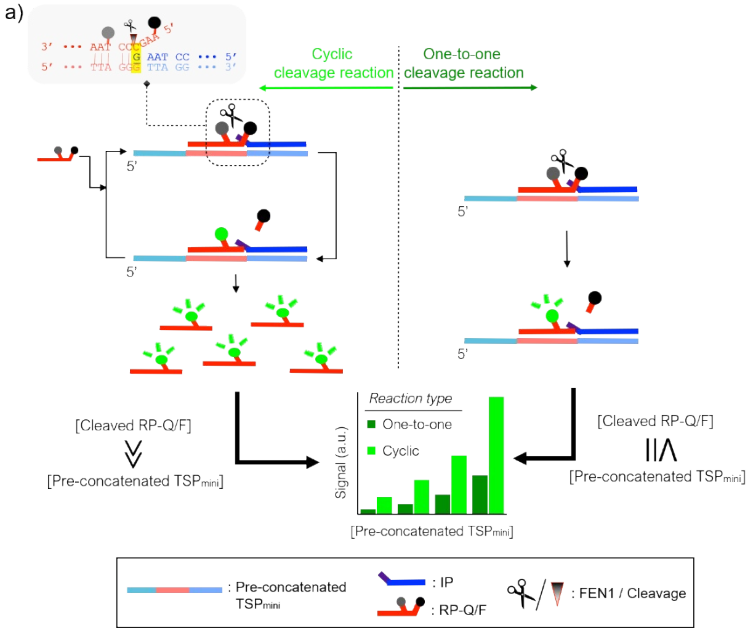

b)

Probe[a]	Sequence (5' — 3')
Pre-concatenated TSP_{mini}	AAT CCG TCG AGC AGA GTT AGG GTT AGG GTT AGG GTT AGG GTT A
IP[b]	CCC TAA CCC TAA G
RP-Q/F[c]	BHQ1-AAG CCC T(F)AA CCC TAA
RP_{cut}-F[c]	CCT(F) AAC CCT AA

[a] The colors of oligonucleotide sequences correspond to those of the domains depicted in **Fig. S2(a)**.
[b] Underlined base invades the junction site (gray box, **Fig. S2(a)**).
[c] F indicates an internal fluorophore in which FAM was used.

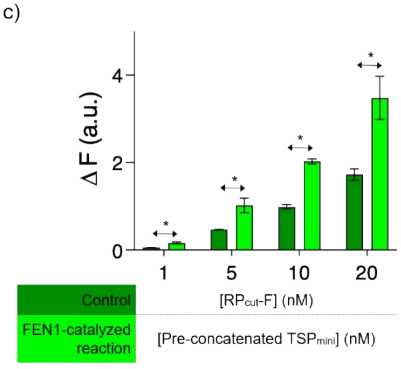

Fig S3. Optimization of reaction concentrations. Varying concentrations of key assay components were tested in the absence and presence of HeLa cell extracts (10^4 cells). We compared signal-to-noise ratios (SNRs) and selected optical concentrations of RP (a), IP (b), FEN1 (c), GO (d), and dNTP (e).

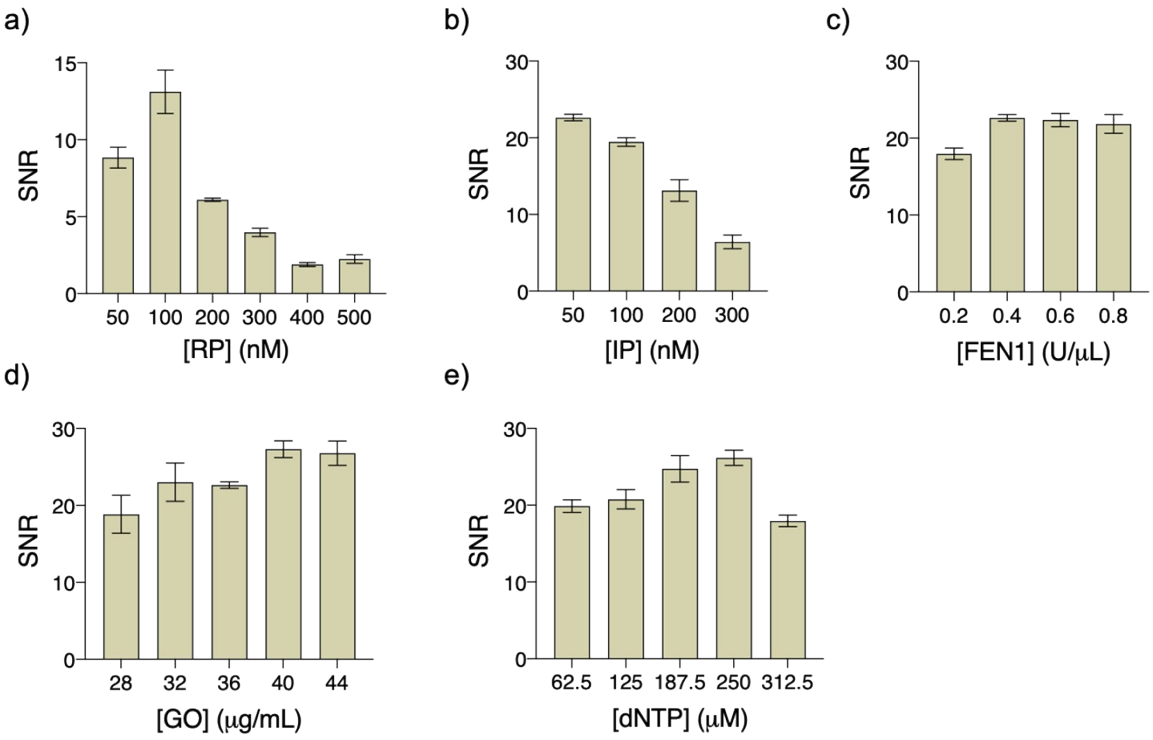

Fig S4. Optimization of reaction times. To minimize the assay time, we tested different times in the absence and presence of HeLa cell extracts (10^4 cells). Comparing SNRs, we found optimal times for QUEST reaction (a) and GO-aided BG filtering (b).

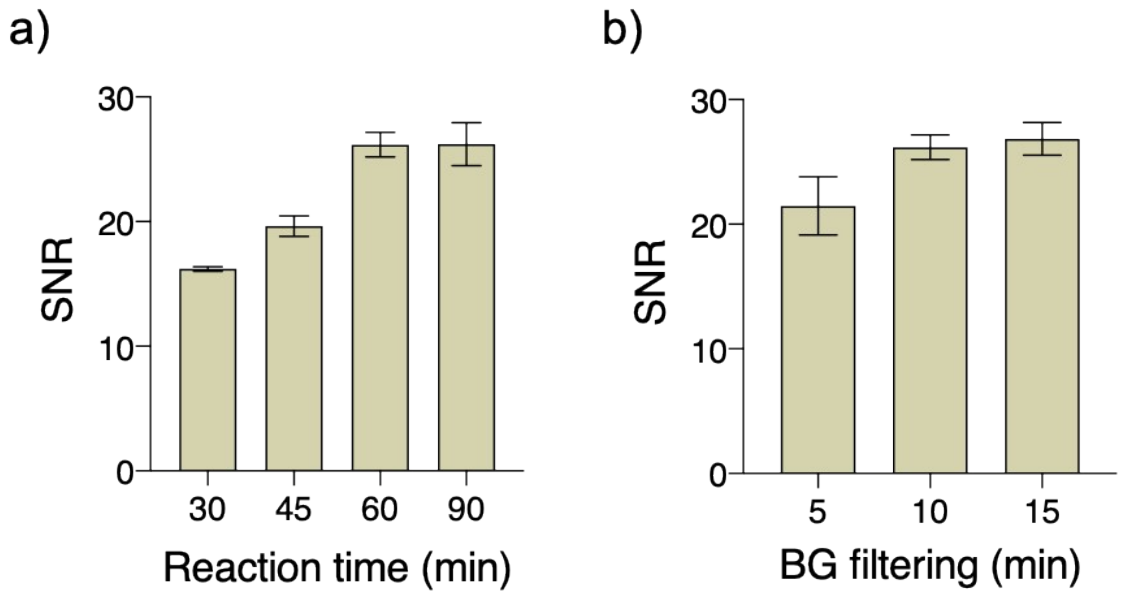

Fig S5. TRAP for telomerase activity assay for various cell lines. The telomerase activities in various cell lines were analyzed by TRAP, the standard method for telomerase activity assay. The results matched with those in Fig. 3, supporting the reliability of QUEST. [Cell extract]: 10^4 cells. BL: Blank, where cell extract was not added.

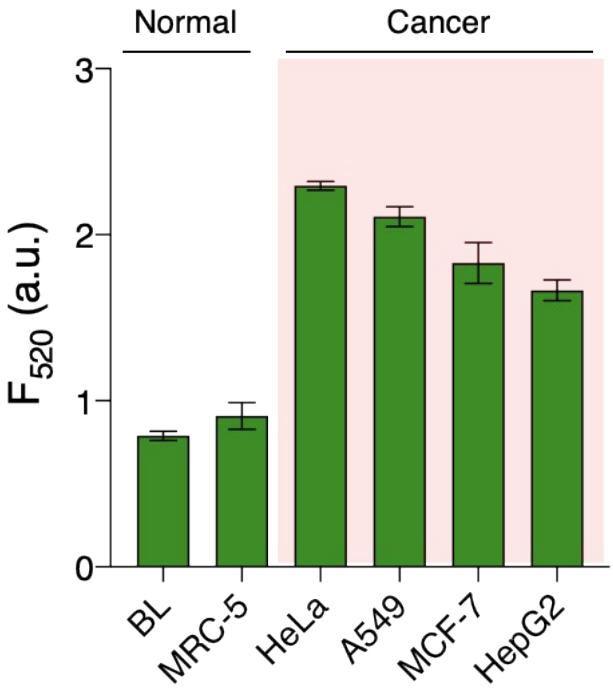

Fig S6. Effect of AZT on QUEST reaction. (a) To make sure that AZT does not affect other parts of QUEST from telomerase activity, we investigated the QEUST reaction in the presence of AZT (10 nM). For this, we used the pre-concatenated TSP (100 nM), which is TSP appended with telomeres ($(TTAGGG)_{12}$), while excluding TSP and HeLa cell extract. (b) SNRs were obtained from the results in (a) and normalized to directly elucidate the effect of AZT on QUEST reaction. The effect was negligible as indicated by *p* value higher than 0.05.

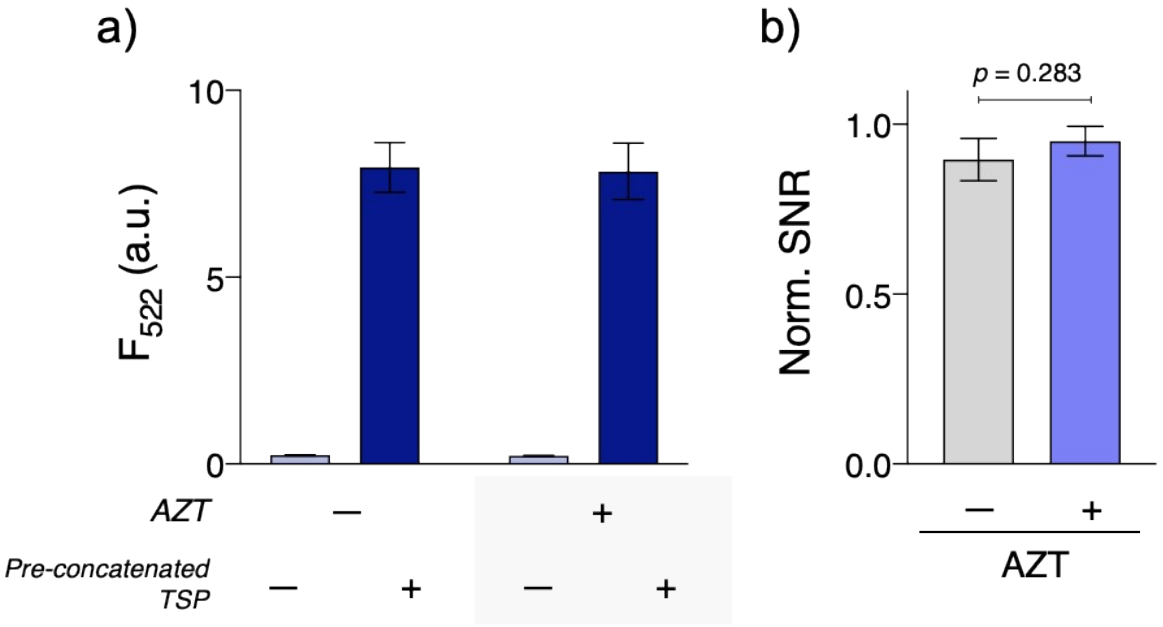

Fig S7. GO Characterization. (a) AFM image and (b) topographic profile of GO.

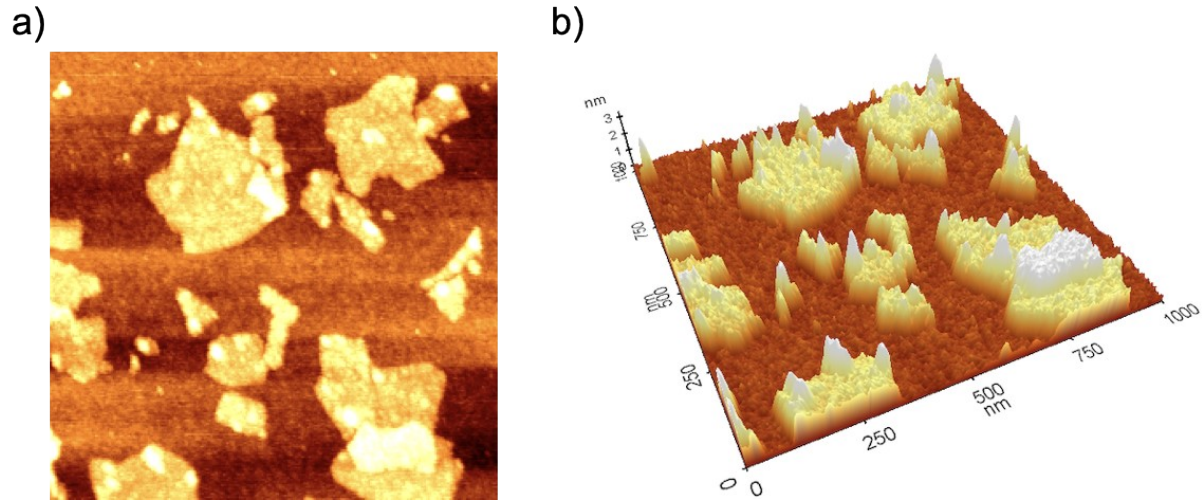

Table S1. Comparison with previous telomerase activity assays.

System	Mode	Time (min)	LOD	Cost ($/assay)	Characteristics	Ref
Proximity-induced DNA walker	Electrochemiluminescence	160	16 cells/mL	> 8.45	• Electrode preparation • Nanomaterial preparation and its modification with DNA probes • Washing/separation	5
Catalytic hairpin assembly (CHA) for Au nanorod etching	Surface plasmon resonance	175	15 cells	1.97	• Preparation of nanomaterial • Several steps	6
Entropy-driven circuit reaction and CHA for SERS detection	Surface enhanced Raman spectroscopy	200	1 cell	4.84	• Film fabrication • Nanomaterial preparation and its modification with DNA probes • Several steps accompanying washing/separation	7
DNA network formation	Electrochemistry	> 190	20 cells/mL	> 60	• Electrode preparation and modification with DNA probes • Several steps accompanying washing/separation	8
Dual-DNA walkers on CHA and DNAzyme	Fluorescence	180	7 cells/mL	1.86	• Nanomaterial preparation and its modification with DNA probes	9
3D-bipedal DNA walker	Fluorescence	160	5 cells/mL	11.0	• Nanomaterial preparation and its modification with DNA probes • Intracellular imaging	10
Tetrahedral DNA nanoconjugate	Fluorescence	60	6 cells	N/A	• Nanomaterial preparation and its modification with DNA probes • Intracellular imaging	11
Molecular machine	Fluorescence	180	510 cells/mL	25.8	• Extensive labeling with F and Q • Ratiometric signaling	12
DNA tetrahedron FRET sensor	Fluorescence	60	1 cell	303.8	• Dual probe labeling with F and Q • Intracellular imaging	13
Strand displacement amplification and rolling circle amplification	Fluorescence	120	60 cells/mL	3.62	• Likelihood of non-specific reactions	14
Stem-loop primer-mediated exponential amplification	Fluorescence	105	10^3 cells/mL	1.52	• Likelihood of non-specific reactions • Complicated DNA probe design	15
CRISPR/Cas assay for TRAP product	Colorimetry	180	1 cell	> 2.47	• Need of thermocycling and relevant instrument • Nanomaterial preparation and its modification with DNA probes	16
Elongation-triggered CRISPR/Cas reaction	Fluorescence	60	260 cells/mL	11.5	• Dual probe labeling with F and Q	17
Lateral flow analysis of CRISPR/Cas reaction	Colorimetry	> 65	10^4 cells/mL	4.58	• Need of costly, laborious LFA toolkit • Subjective, qualitative LFA result • Several manual steps	18
QUEST	**Fluorescence**	**70**	**2 cells**	**0.73**	**-**	**-**

(Our work)	**(36 cells/mL)**	

Table S2. Oligonucleotide sequences used in this work.

Purpose	Probe[a]	Sequence (5'—3')
QUEST	TSP	AAT CCG TCG AGC AGA GTT
	RP	FAM-AAG CCC TAA CCC TAA
	IP[b]	CCC TAA CCC TAA G
Gel electrophoresis	RP-Q/F[c]	BHQ1-AAG CCC T(F)AA CCC TAA
Effect of inhibitor on QUEST	Pre-concatenated TSP	AAT CCG TCG AGC AGA GTT AGG GTT AGG GTT AGG GTT AGG GTT AGG GTT AGG GTT AGG GTT AGG GTT AGG GTT AGG G

[a] The colors of oligonucleotide sequences correspond to those of the domains depicted in Scheme 1.
[b] Underlined base invades the junction site (light gray box, **Scheme 1**).
[c] F indicates an internal fluorophore in which FAM was used.

References

1 C. Y. Lee, H. Jang, H. Kim, Y. Jung, K. S. Park and H. G. Park, *Microchim. Acta*, 2019, **186**, 1-7.

2 S. Chen, Z. Xie, W. Zhang, S. Zhao, Z. Zhao, X. Wang, Y. Huang and G. Yi, *Anal. Chim. Acta*, 2023, **1238**, 340653.

3 J. Park, J. Kim, C. Park, J. W. Lim, M. Yeom, D. Song, E. Kim and S. Haam, *Analyst*, 2022, **147**, 5028–5037.

4 S. Ding, Y. Wei, G. Chen, F. Du, X. Cui, X. Huang, Y. Yuan, J. Dong and Z. Tang, *Anal. Chem.*, 2022, **94**, 13549–13555.

5 Y. Guo, S. Liu, H. Yang, P. Wang and Q. Feng, *Anal. Chim. Acta*, 2021, **1144**, 68–75.

6 D. Wang, R. Guo, Y. Wei, Y. Zhang, X. Zhao and Z. Xu, *Biosens. Bioelectron.*, 2018, **122**, 247–253.

7 Y. Li, H. Han, Y. Wu, C. Yu, C. Ren and X. Zhang, *Biosens. Bioelectron.*, 2019, **142**, 111543.

8 L. Liu, D. Wu, S. Zhen, K. Lu, X. Yi and Z. Sun, *Sens. Actuators B: Chem.*, 2021, **334**, 129659.

9 Y. Shen, J. Gong, S. Li, C. Liu, L. Zhou, J. Sheng and X. Qingxia, *Sens. Actuators B: Chem.*, 2021, **329**, 129078.

10 F. Meng, H. Chai, X. Ma, Y. Tang and P. Miao, *J. Mater. Chem. B*, 2019, **7**, 1926–1932.

11 X. Liu, F. Meng, R. Sun, K. Wang, Z. Yu and P. Miao, *Chem. Commun.*, 2021, **57**, 2629–2632.

12 C. He, Z. Liu, Q. Wu, J. Zhao, R. Liu, B. Liu and T. Zhao, *ACS Sensors*, 2018, **3**, 757–762.

13 C. Jiang, F. Meng, D. Mao, Y. Tang and P. Miao, *ChemBioChem*, 2021, **22**, 1302–1306.

14 F. Ma, S. H. Wei, J. Leng, B. Tang and C. Y. Zhang, *Chem. Commun.*, 2018, **54**, 2483–2486.

15 H. Wang, H. Wang, C. Liu, X. Duan and Z. Li, *Chem. Sci.*, 2016, **7**, 4945–4950.

16 M. Cheng, E. Xiong, T. Tian, D. Zhu, H. qiang Ju and X. Zhou, *Biosens. Bioelectron.*, 2021, **172**, 112749.

17 P. Yu, T. Yang, D. Zhang, L. Xu, X. Cheng, S. Ding and W. Cheng, *Anal. Chim. Acta*, 2021, **1159**, 338404.

18 X. Chen, Y. Deng, G. Cao, X. Liu, T. Gu, R. Feng, D. Huo, F. Xu and C. Hou, *Anal. Chim. Acta*, 2021, **1146**, 61–69.